NJC

PAPER

View Article Online
View Journal | View Issue

Cite this: *New J. Chem.*, 2017, **41**, 9668

Phenothiazine based blue emitter for light-emitting electrochemical cells†

Kanagaraj Shanmugasundaram,[a] Ramesh Kumar Chitumalla,[b] Joonkyung Jang[b] and Youngson Choe*[a]

Received 24th March 2017,
Accepted 24th July 2017

DOI: 10.1039/c7nj00976c

rsc.li/njc

A butterfly shaped phenothiazine based electroluminescent material **PPPSO2** was synthesized as an ionic small molecule emitter for light-emitting electrochemical cells (LECs). **PPPSO2** shows deep blue emission in solution with high fluorescent quantum yield of 0.49. By employing the active molecule **PPPSO2** as an emitter in LECs, the device shows electroluminescence centered at 498 nm with CIE coordinates of (0.21, 0.31) and maximum luminance of 509 cd m^{-2}. The results show that the versatility of phenothiazine based luminescent materials such as high thermal stability and different emission color by tuning the oxidation state makes phenothiazine derivatives a prospective material for light-emitting devices.

Introduction

Increased concerns over global warming caused by inefficient lighting has driven research into finding efficient lighting sources. As such, the development of organic electronics can be a solution to reduce global warming to some extent. For the last two decades, studies have been focused on organic light-emitting diodes (OLEDs), and efficient OLEDs have now entered into the display market.[1] However, the most efficient OLEDs are based on multi-stack devices developed from the sequential evaporation of the active materials under vacuum, which leads to high device cost. The multi-layers are responsible for charge injection and transport in the OLED devices; the utilization of OLEDs in general lighting application is not yet feasible due to their considerably high manufacturing cost. Pei *et al.* introduced single-layered electroluminescent devices, called light-emitting electrochemical cells (LECs), which have simple device architectures, utilize air stable electrodes, and a single active layer is responsible for both light-emission and charge transport.[2] Electronic charge transport in LEC devices is achieved by mobile ions present in the active layer, which makes LECs a better alternative to OLEDs. Active layers in LEC devices can be fabricated from an inexpensive solution-processing spin-coating method. Thus, LECs have been receiving increasing research interest with respect to fabricating efficient low-cost light-emitting devices. Recently, Edman *et al.* have shown a low-cost and efficient scalable method for fabricating cost-efficient LEC devices.[3,4] The light-emitting materials in LECs are either ionic-transition metal complexes (iTMCs)[5–7] or neutral light-emitting polymers.[8–10] The iridium metal complexes were well explored due to their high stability and intrinsically higher photoluminescence efficiencies.[11–19] Despite the efficient performance of iridium-iTMC LECs, the low abundance and high cost of iridium leads to an increase in the overall device cost for large scale applications. Recently, neutral organic small molecules have attracted much attention and found their way into LECs as an active material with polyethylene oxide and an inorganic salt.[20–22] However, these tri-component blends used for charge transport in LECs lead to phase separation in thin films.[2] To overcome the need of tri-component blend, efficient emitters with charge transporting abilities are emerging for LECs. Therefore, ionic organic small molecules are highly desirable materials to facilitate both charge transport and emitting role in LECs. Recently, charged organic small molecules were successfully utilized as an active material and served dual roles in LECs.[23–31] Unique potential features of phenothiazine materials were beneficial for optoelectronic application and successfully applied in dye-sensitized solar cells and solid-state lighting devices.[32–36] Recently, we reported for the first time a charged phenothiazine derivative based green LEC.[37] The obtained results with the sulfide form of phenothiazine derivative shows the ability of phenothiazine materials to function as an active layer in single component LEC devices.

In this study, we report the synthesis and characterization of the sulfone form of a charged phenothiazine derivative. The increased oxidation state of the molecule resulted in higher thermal stabilities compared to that of its parent molecule, and the emission spectra showed a hypsochromic shift relative to that of their sulfide derivative.[37] As a result, the high thermal

[a] *School of Chemical and Biomolecular Engineering, Pusan National University, Busan 609-735, Republic of Korea. E-mail: choe@pusan.ac.kr; Fax: +8251 512 8634; Tel: +8251 510 2396*
[b] *Department of Nanoenergy Engineering, Pusan National University, Busan, 609-735, Republic of Korea*

† Electronic supplementary information (ESI) available. See DOI: 10.1039/c7nj00976c

stability and reasonable photophysical properties suggest that the sulfone form of phenothiazine derivatives would be beneficial for LEC device application. Single-component LEC devices were fabricated with sulfone derivative by solution processing method. LEC devices employing **PPPSO2** as active material show maximum brightness of 509 cd m^{-2} and current density of 83 mA cm^{-2} at 7.5 V.

Experimental

General information

All reagents and solvents used for synthesis were purchased from commercial suppliers and were used as received without further purification. ^{1}H spectra were measured on Varian unity Inova-300 MHz spectrometer with tetramethylsilane (TMS) as the internal standard. The glass transition temperature (T_g) of the compound was measured using differential scanning calorimetry (DSC) under a nitrogen atmosphere at a heating rate of 10 °C min^{-1} with TA instruments Q200. The glass transition temperature (T_g) was determined from the second heating scan. Thermogravimetric analysis (TGA) was performed using a Netzsch TG 209 instrument under N_2 flow at a heating rate of 10 °C min^{-1}. Ultraviolet-visible absorption spectra were measured with a UV-VIS spectrometer, Lamda-20, PerkinElmer spectrophotometer. Fluorescence measurements were carried out with Hitachi F-7000 FL spectrophotometer. Photoluminescence quantum yield (PLQY) was measured in toluene solution using 9,10-diphenylanthracene as a standard. The optical band gap (E_g) was obtained from the onset potential of an absorption spectrum. Transient PL of the material was measured using a compact fluorescence lifetime spectrometer C11367 at room temperature. The electrochemical measurements were performed on cyclic voltammetry (CV) model of potentiostat/galvanostat (Iviumstat) voltammetric analyzer with platinum working electrode and platinum wire counter electrode at a scanning rate of 100 mV s^{-1} against Ag/AgCl as the reference electrode. Acetonitrile was employed as the solvent with 0.1 M tetra-*n*-butylammonium hexafluorophosphate ($TBAPF_6$) as the supporting electrolyte. The HOMO energy level of the molecule was calculated from the estimated onset potential of oxidation using the formula $E_{HOMO} = -4.40 - E_{onset}(ox)$ and the LUMO were obtained by summing the E_g to the calculated HOMO energy level.

Synthesis

The synthetic routes of the intermediates and target compound are displayed in Scheme 1. The intermediate 3,6-dibromo-10-(6-bromohexyl)-10*H*-phenothiazine (**1**) was synthesized according to the previous report.[37] Structures of **PPP** and **PPPSO2** are given Fig. S1 (ESI†).

Synthesis of 2. To a stirred solution of compound **1** (1 g, 3.84 mmol) in 60 mL dichloromethane (CH_2Cl_2) was added excess *m*-chloroperoxybenzoic acid (*m*-CPBA) at 0 °C. The resulting reaction mixture was stirred for 4 h under inert atmosphere. After completion of reaction, excess *m*-CPBA was removed by washing with 2 M K_2CO_3 solution. The reaction mixture was extracted with DCM and dried over Na_2SO_4. The resultant crude product was purified by column chromatography on silica gel eluted with hexane/ethyl acetate to offer off-white solid of **2**. Yield: 64%. ^{1}H NMR (300 MHz, $CDCl_3$, δ): 8.21–8.16 (s, 2H), 7.74–7.64 (d, 2H), 7.28–7.16 (d, 2H), 4.20 (t, 2H), 3.40 (t, 2H), 1.95–1.82 (m, 4H), 1.61–1.40 (m, 4H).

Synthesis of 3. Compound **2** (0.50 g, 0.91 mmol), 1-pyreneboronic acid (0.56 g, 2.27 mmol), $Pd(PPh_3)_4$ (0.04 g, 0.04 mmol), TBAB (0.03 g, 0.10 mmol) and K_2CO_3 (0.69 g, 5.00 mmol) were added to 2 : 1 (v/v) mixture of tetrahydrofuran/water under argon atmosphere. The reaction mixture was stirred at 70 °C for 24 h. Upon completion of the reaction, the mass was cooled to RT, and the mixture was extracted with dichloromethane and dried over Na_2SO_4. The solvent was concentrated under reduced pressure, and the residue was purified by column chromatography on silica gel eluted with *n*-hexane/ethyl acetate (7/3; v/v) to afford compound **3** as off-white solid. Yield: 72%. ^{1}H NMR (300 MHz, $CDCl_3$, δ): 8.52–8.45 (m, 2H), 8.32–7.88 (m, 20H), 7.64–7.30 (m, 2H), 4.40 (t, 2H), 3.45 (t, 2H), 2.20–1.90 (m, 4H), 1.70–1.50 (m, 4H).

Synthesis of PPPSO2. To a solution of compound **3**, (0.50 g, 0.63 mmol) in 5 mL toluene was added excess 1-methylimidazole (2 mL), and the resulting reaction mixture was stirred to reflux for overnight under argon atmosphere. After completion of reaction, the mass was concentrated and the final product was obtained by adding saturated KPF_6 solution and stirred for 2 h. Then, the resulting solid was filtered, washed several times with water and hexane and dried in vacuum at 45 °C for 16 h. The product was purified by recrystallization in DCM with

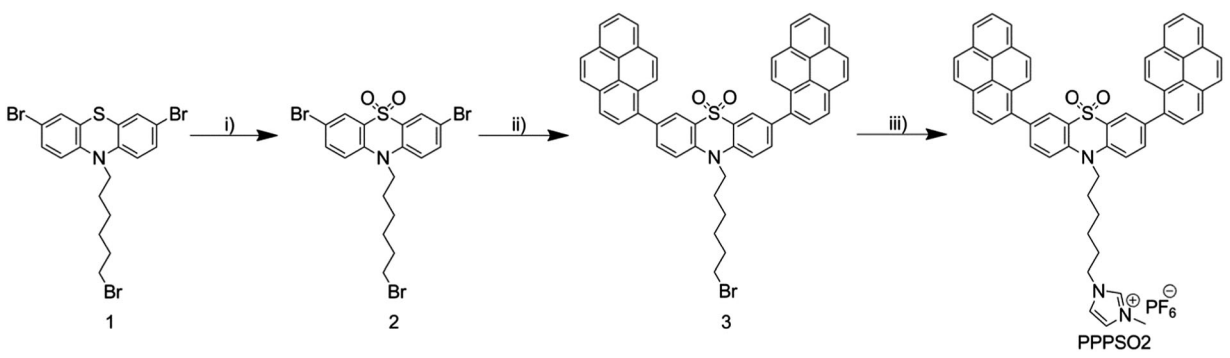

Scheme 1 (i) *m*-CPBA, DCM. (ii) $Pd(PPh_3)_4$, TBAB, K_2CO_3, THF/H_2O. (iii) 1-Methylimidazole, toluene.

diethyl ether to afford pure **PPPSO2**. Yield: 76%. ^{1}H NMR (Fig. S2, ESI†) (300 MHz, d_6-DMSO, δ): 9.10–9.04 (s, 1H), 8.44–8.14 (m, 13H), 8.14–7.94 (m, 11H), 7.78–7.72 (s, 1H), 7.68–7.62 (s, 1H), 4.50 (t, 2H), 4.15 (t, 2H), 3.80 (s, 3H), 2.00–1.75 (m, 4H), 1.60–1.28 (m, 4H).

Device fabrication

Before the fabrication of the devices, indium tin oxide (ITO)-coated glass substrates were carefully cleaned with acetone, ethanol and isopropyl alcohol in an ultrasonic bath. Then, they were dried in an oven at 120 °C for 30 minutes. After drying, PEDOT:PSS (poly(3,4-ethylenedioxythiophene)–poly(styrene sulfonate)) layer was spin-coated onto ITO anode and annealed at 120 °C. The light-emitting layer was spin coated onto the PEDOT/PSS layer by spin-coating from acetonitrile solution and annealed at 80 °C for 1 h in vacuum. The cathode contacts were fabricated by thermal evaporation of the aluminum on top of the active layer at high vacuum using a shadow mask. Electroluminescence spectra and CIE coordinates were measured using an Avantes luminance spectrum. The current density and luminance *versus* driving voltage characteristics were measured with a Keithley 2400 source meter coupled with an OPC 2100 optical spectrum analyzer in ambient atmosphere.

Results and discussions

Thermal properties

Thermal properties of **PPPSO2** were studied using thermogravimetric analysis (TGA) and differential scanning calorimetry (DSC) under nitrogen flow at a scanning rate of 10 °C min^{-1} (Fig. 1).

The decomposition temperature (T_d, corresponding to 5% weight loss) of **PPPSO2** was high as 390 °C, and it also showed a high glass transition temperature (T_g) of 154 °C. The relatively high glass transition temperature of the compound resulted in stable glasses in its film state. The thermal data is summarized in Table 1. The results of TGA and DSC revealed that the compound **PPPSO2** possessed higher thermal stability than **PPP**.[37] The rigid molecular conformation of **PPPSO2** offers higher thermal stability, and thus a higher T_g. This clearly highlights that the increase in the oxidation state shows an increase in rigidity, thereby enhancing the thermal stability of the compound. The good thermal stability and high glass transition temperature were prerequisite to form morphologically stable film for their application in LECs.

Table 1 Photophysical and thermal properties of **PPP** and **PPPSO2**

Compound	$\lambda_{UV,max}$[a] (nm)	$\lambda_{PL,max}$[a] (nm)	$\lambda_{UV,max}$[b] (nm)	$\lambda_{PL,max}$[b] (nm)	Φ_f[c]	τ[d] (ns)	E_g[e] (eV)	T_d[f] (°C)
PPP	345	507	349	514	0.10/0.03	1.15	2.92	355
PPPSO2	350	410	358	463	0.49/0.11	1.14	3.15	390

[a] Measured in toluene (10^{-5} M). [b] Measured in thin-film. [c] Photoluminescence quantum yield (PLQY) in toluene and thin film. [d] Lifetime of fluorescence as determined in toluene solution. [e] Optical band gap calculated from onset of absorption spectrum. [f] Thermal decomposition (T_d) temperature.

Photophysical properties

Optical properties of **PPPSO2** were evaluated by measuring UV-visible absorption and photoluminescence spectra in toluene solution, and the results are shown in Fig. 2. **PPPSO2** showed absorption bands at 300–350 nm, which were assigned to the π–π* transition of the molecular backbone.

The optical energy gap of **PPPSO2** was estimated to be 3.15 eV as calculated from the onset of the absorption spectrum. The emission maximum of **PPPSO2** in toluene solution was located at 410 nm. The fluorescence quantum yield of **PPPSO2** was found to be 0.49, which is 5-times higher than the previously reported molecule.[37] It revealed that the oxidized sulfur form of the molecule shows enhanced quantum yield. The absorption and photoluminescence spectra in the thin films are displayed in Fig. S3 (ESI†). It shows red-shifted emission spectrum up to 53 nm compared to its solution emission spectrum, clearly implying the presence of intermolecular interactions.

However, both the emission spectra of **PPPSO2** in solution as well as in thin film were blue-shifted compared to its

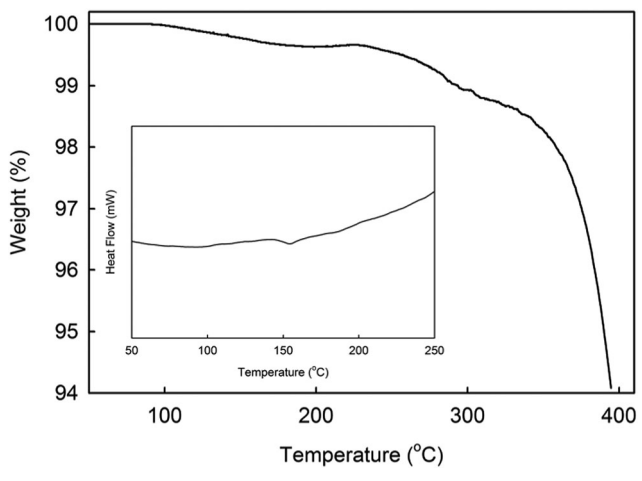

Fig. 1 TGA curve (inset: DSC curve) of **PPPSO2**.

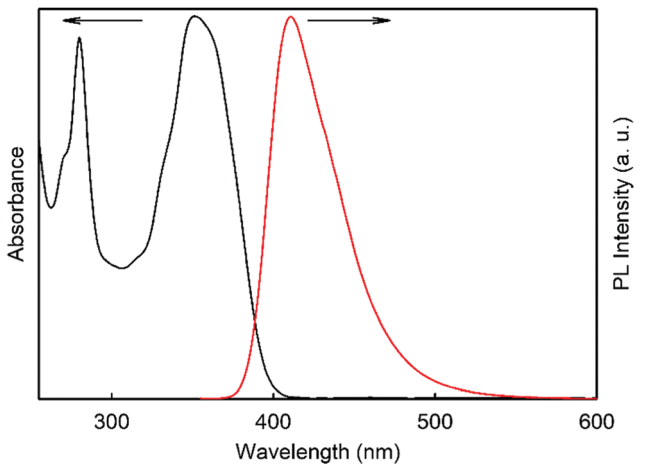

Fig. 2 UV-visible absorption and PL spectrum of **PPPSO2** in toluene solution.

congener **PPP**.[37] The observed blue-shift results from the configural distinction at the excited state of the molecules.[35] In the thin film, low quantum yield was observed due to the presence of intermolecular interactions, which led to quench the emission intensity.[38] Fig. S4 (ESI†) represents the transient photoluminescence spectrum of the compound in an oxygen-free toluene solution. We investigated the low temperature PL spectrum to measure the triplet energy of the compound. However, we could not observe any characteristic peaks in the spectrum. The spectrum shows that the compound does not have triplet excited state. Lifetime of the molecule was calculated from the transient PL spectrum to be 1.14 ns. To investigate the excited state nature of the emitter, PL spectra were measured with different solvents, and the observed solvatochromic effects are shown in Fig. S5 (ESI†). The gradual bathochromic shift of 24 nm with increasing solvent polarity suggested the presence of charge transfer character in the emitter. However, the obtained shift was lower than that of the previously reported emitter **PPP**. This decrease in CT character clearly comes from the lower donating ability of the emitter, because the introduction of sulfone unit lowers the donating ability of phenothiazine of **PPPSO2** compared with **PPP**.[37]

Electrochemical properties

CV measurements were performed to ascertain the oxidation potential of the target material in acetonitrile solution as shown in Fig. 3. The energy levels of **PPPSO2** were estimated using cyclic voltammetry and UV-visible absorption.

From the onset potential of oxidation (0.89 V), the HOMO energy level of molecule was calculated and it was found to be −5.29 eV. It can be seen that the HOMO level of sulfone derivative was reduced compared to that of the previously reported **PPP** due to the electron affinity of sulfone unit.[37]

The LUMO energy level was calculated by subtracting the optical energy gap from the HOMO energy level of the compound. The calculated LUMO energy level was found to be −2.14 eV for **PPPSO2**. Compared with the analogous molecule **PPP**, reduced HOMO and LUMO energy levels were obtained due to strong electron affinity of sulfone unit in the molecule. The results revealed that a change in the oxidation state of sulfur lowers the HOMO energy level of the molecule. All the physical properties data are summarized in Table 1.

Theoretical investigations

To study the structure–property relationship of the compound at a molecular level, density functional theory (DFT) calculations were performed using B3LYP[39–41] hybrid functional at 6-31G(d) basis set for **PPPSO2**.

The optimized structure of **PPP** has non planar geometry with a butterfly shape, as shown in Fig. S6 (ESI†). The observed bond angles at sulfur (99.5°) and at nitrogen (121.2°) were in good agreement with the previously reported results.[35,37] The pyrene groups in the molecule do not share the same plane with the phenothiazine ring, and this concludes that the molecule has a twisted and rigid structure. The molecular orbitals of **PPPSO2** are shown in Fig. 4. The HOMO of **PPPSO2** was confined at the phenothiazine and pyrene moieties, and the LUMO was located on the pyrene rings. The HOMO and LUMO energy levels were eventually distributed, ensuring high quantum yield and a weak charge transfer feature due to little differences in the electron density contours compared to the previous report.[37] The calculated HOMO (−5.33 eV) of **PPPSO2** was similar to that of experimentally obtained value, whereas the LUMO energy level was calculated to be −1.88 eV. The TDDFT method was performed to obtain the UV-visible absorption spectrum of the compound **PPPSO2**. The TDDFT results obtained from the simulations are compiled in Table S1 (ESI†), and the absorption spectrum is depicted in Fig. S7 (ESI†). As shown in Fig. S7 (ESI†), the TDDFT simulations reproduced the main bands that were observed in the experimental spectrum. The simulated low energy absorption peak was observed at 340 nm, which is in agreement with the experimental absorption maxima at 350 nm. The low energy absorption occurred mainly due to the transitions from HOMO to LUMO (50%).

Electroluminescence properties

TGA and DSC measurements show that the compound has high thermal stability and indicates its stable film forming ability to fabricate electroluminescent devices. To investigate the

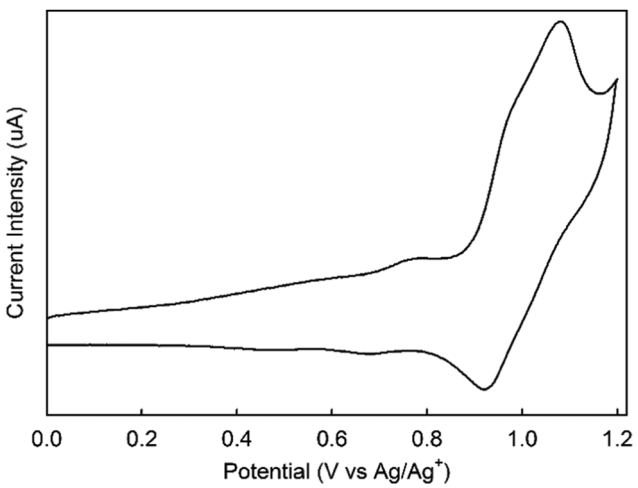

Fig. 3 Cyclic voltammogram of **PPPSO2**.

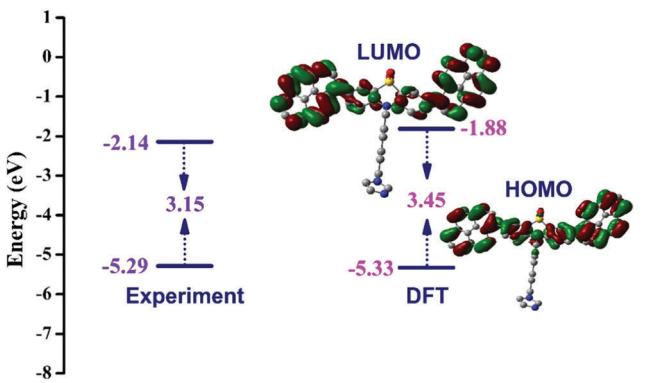

Fig. 4 Electron density distribution and comparison of energy levels.

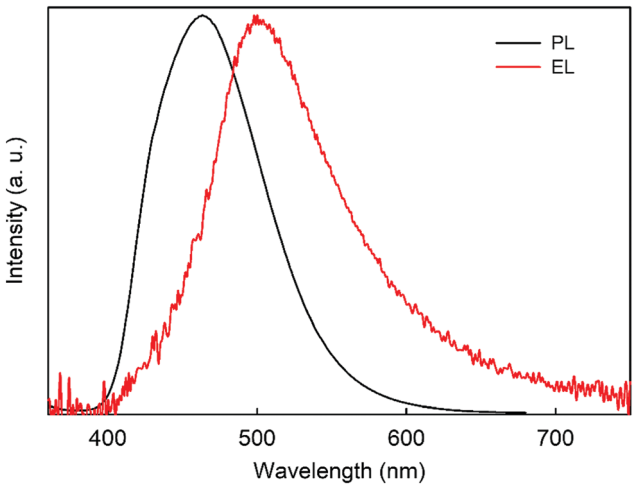

Fig. 5 EL spectra of the devices in comparison with thin-film PL spectra of the compound.

potential of **PPPSO2** as an emitter in LECs, the electroluminescent devices were fabricated with the configuration of ITO/PEDOT:PSS/**PPPSO2**/Al. The light-emitting layer was processed from acetonitrile solution, and the EL spectra (Fig. 5) of the devices exhibited an emission band maximum at 498 nm. The observed CIE coordinates of (0.21, 0.31) indicated sky-blue emission of the compound. In comparison with the thin-film photoluminescence spectrum, the observed electroluminescence spectrum was red-shifted up to 35 nm due to the intermolecular interaction as well as polarization effect of molecular orbitals under electric field in the LEC devices (Table 2).[42]

However, **PPPSO2** exhibited blue shifted EL spectrum compared to the EL spectrum of **PPP**.[37] Fig. 6 shows the current density–voltage–brightness (*J*–*V*–*L*) curves of the fabricated devices.

The devices showed a maximum brightness of 509 cd m^{-2} and maximum current density of 83 mA cm^{-2} at a voltage of 7.5 V. The low brightness of the devices is consistent with low thin film quantum yields of the compound.[38] The fabricated device exhibited a higher turn-on voltage (V_{on}) (at a brightness of 1 cd m^{-2}) of 4.8 V for **PPPSO2** compared with 4.0 V for **PPP**. Sulfone derivatives of the compound show sky-blue emission in the electroluminescent devices, whereas the sulfide derivatives exhibit green emission in the EL devices. As a result, the sulfone derivative displayed different photophysical and electroluminescence properties compared with sulfide derivative. This study revealed that by changing the oxidation state of sulfur in the molecule, the emission color of the compound can be tuned to the sky-blue region.

Table 2 EL characteristics of the devices

Compound	EL_{max} [a]	V_{on} [b] (V)	L_{max} [c] (cd m^{-2})	CIE (*x*, *y*) [d]
PPP	530	4.0	499	(0.32, 0.58)
PPPSO2	498	4.8	509	(0.21, 0.31)

[a] Maximum luminescence. [b] Turn-on voltages at 1 cd m^{-2}. [c] Maximum efficiency (brightness in cd m^{-2} at maximum efficiency is in parentheses). [d] Commission International de I'Eclairage coordinates (CIE) measured at 50 mA.

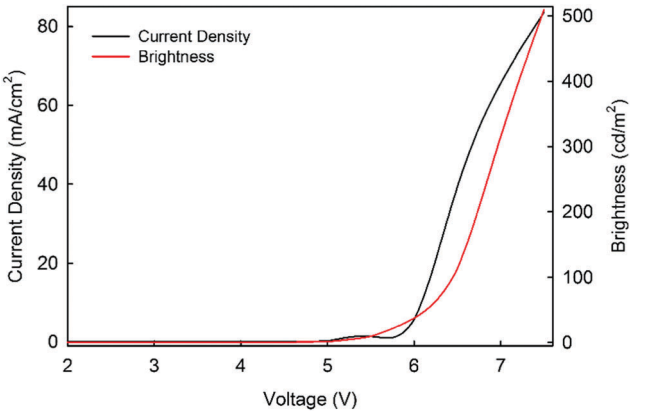

Fig. 6 Current density–voltage–luminance (*J*–*V*–*L*) characteristics of the devices.

Conclusions

We have designed and synthesized an electroluminescent material with a butterfly structure based on phenothiazine core with pyrene moieties. The phenothiazine sulfur atom was oxidized into sulfone. Incorporation of the sulfone unit blue shifted the emission profile of the compound and showed improved fluorescence quantum yields over the previously studied molecule **PPP**. The resulting chromophore **PPPSO2** shows small solvatochromism and typically a high thermal stability. Non-doped single-layer electroluminescent devices were fabricated by incorporating **PPPSO2** as an emitter. The devices display EL emission centered at 498 nm with the CIE coordinates of (0.21, 0.31). As a result of oxidation of the sulfur atom in the molecule pulls the electroluminescence towards the blue region. This study reveals that the strategy of phenothiazine based derivatives by changing the oxidation state of the molecules is capable of providing effective approach to construct low-cost full color displays.

Acknowledgements

This research has been supported by the Basic Science Research program through the National Research Foundation of Korea (NRF) financial support by Ministry of Education, Science and Technology (NRF-2016R1D1A1B02013505) and Brain Korea 21 Plus project.

Notes and references

1 S. Reineke, F. Lindner, G. Schwartz, N. Seidler, K. Walzer, B. Lussem and K. Leo, *Nature*, 2009, **459**, 234–238.
2 Q. Pei, G. Yu, C. Zhang, Y. Yang and A. J. Heeger, *Science*, 1995, **269**, 1086–1088.
3 A. Sandstrom, H. F. Dam, F. C. Krebs and L. Edman, *Nat. Commun.*, 2012, **3**, 1002–1006.

4 A. Sandstrom, A. Asadpoordarvish, J. Enevold and L. Edman, *Adv. Mater.*, 2014, **26**, 4975–4980.
5 R. D. Costa, E. Ortí and H. J. Bolink, *Pure Appl. Chem.*, 2011, **83**, 2115–2128.
6 B. N. Bideh, C. Roldán-Carmona, H. Shahroosvand and M. K. Nazeeruddin, *Dalton Trans.*, 2016, **45**, 7195–7199.
7 D. A. W. Ross, P. A. Scattergood, A. Babaei, A. Pertegás, H. J. Bolink and P. I. P. Elliott, *Dalton Trans.*, 2016, **45**, 7748–7757.
8 S. Tang, H. A. Buchholz and L. Edman, *ACS Appl. Mater. Interfaces*, 2015, **7**, 25955–25960.
9 Y. Nishikitani, H. Takeuchi, H. Nishide, S. Uchida, S. Yazaki and S. Nishimura, *J. Appl. Phys.*, 2015, **118**, 225501.
10 Y. Nishikitani, D. Takizawa, H. Nishide, S. Uchida and S. Nishimura, *J. Phys. Chem. C*, 2015, **119**, 28701–28710.
11 A. M. Bunzli, E. C. Constable, C. E. Housecroft, A. Prescimone, J. A. Zampese, G. Longo, L. Gil-Escrig, A. Pertegas, E. Orti and H. J. Bolink, *Chem. Sci.*, 2015, **6**, 2843–2852.
12 C. D. Sunesh, K. Shanmugasundaram, M. S. Subeesh, R. K. Chitumalla, J. Jang and Y. Choe, *ACS Appl. Mater. Interfaces*, 2015, **7**, 7741–7751.
13 L. He, J. Qiao, L. Duan, G. F. Dong, D. Q. Zhang, L. D. Wang and Y. Qiu, *Adv. Funct. Mater.*, 2009, **19**, 2950–2960.
14 H. C. Su, C. C. Wu, F. C. Fang and K. T. Wong, *Appl. Phys. Lett.*, 2006, **89**, 261118.
15 T. Hu, L. He, L. Duan and Y. Qiu, *J. Mater. Chem.*, 2012, **22**, 4206–4215.
16 R. D. Costa, F. J. Cespedes-Guirao, E. Orti, H. J. Bolink, J. Gierschner, F. Fernandez-Lazaro and A. Sastre-Santos, *Chem. Commun.*, 2009, 3886–3888.
17 A. B. Tamayo, S. Garon, T. Sajoto, P. I. Djurovich, I. M. Tsyba, R. Bau and M. E. Thompson, *Inorg. Chem.*, 2005, **44**, 8723–8732.
18 R. D. Costa, E. Orti, H. J. Bolink, S. Graber, S. Schaffner, M. Neuburger, C. E. Housecroft and E. C. Constable, *Adv. Funct. Mater.*, 2009, **19**, 3456–3463.
19 D. Tordera, A. Pertegás, N. M. Shavaleev, R. Scopelliti, E. Orti, H. J. Bolink, E. Baranoff, M. Gratzel and M. K. Nazeeruddin, *J. Mater. Chem.*, 2012, **22**, 19264–19268.
20 Z. B. Hill, D. B. Rodovsky, J. M. Leger and G. P. Bartholomew, *Chem. Commun.*, 2008, 6594–6596.
21 S. Tang, W. Y. Tan, X. H. Zhu and L. Edman, *Chem. Commun.*, 2013, **49**, 4926–4928.
22 M. S. Subeesh, K. Shanmugasundaram, C. D. Sunesh, Y. S. Won and Y. Choe, *J. Mater. Chem. C*, 2015, **3**, 4683–4687.
23 H. F. Chen, C. T. Liao, T. C. Chen, H. C. Su, K. T. Wong and T. F. Guo, *J. Mater. Chem.*, 2011, **21**, 4175–4181.
24 H. F. Chen, C. T. Liao, M. C. Kuo, Y. S. Yeh, H. C. Su and K. T. Wong, *Org. Electron.*, 2012, **13**, 1765–1773.
25 A. Pertegás, D. Tordera, J. J. Serrano-Pérez, E. Ortí and H. J. Bolink, *J. Am. Chem. Soc.*, 2013, **135**, 18008–18011.
26 A. Pertegás, N. M. Shavaleev, D. Tordera, E. Ortí, M. K. Nazeeruddin and H. J. Bolink, *J. Mater. Chem. C*, 2014, **2**, 1605–1611.
27 M. Y. Wong, G. J. Hedley, G. Xie, L. S. Kölln, I. D. W. Samuel, A. Pertegás, H. J. Bolink and E. Zysman-Colman, *Chem. Mater.*, 2015, **27**, 6535–6542.
28 K. Shanmugasundaram, M. S. Subeesh, C. D. Sunesh, R. K. Chitumalla, J. Jang and Y. Choe, *Org. Electron.*, 2015, **24**, 297–302.
29 M. S. Subeesh, K. Shanmugasundaram, C. D. Sunesh, T. P. Nguyen and Y. Choe, *J. Phys. Chem. C*, 2015, **119**, 23676–23684.
30 K. Shanmugasundaram, M. S. Subeesh, C. D. Sunesh and Y. Choe, *RSC Adv.*, 2016, **6**, 28912–28918.
31 M. S. Subeesh, K. Shanmugasundaram, C. D. Sunesh, R. K. Chitumalla, J. Jang and Y. Choe, *J. Phys. Chem. C*, 2016, **120**, 12207–12217.
32 Y. Hua, S. Chang, D. Huang, X. Zhou, X. Zhu, J. Zhao, T. Chen, W. Y. Wong and W. K. Wong, *Chem. Mater.*, 2013, **25**, 2146–2153.
33 G. B. Bodedla, K. R. Justin Thomas, S. Kumar, J. H. Jou and C. J. Li, *RSC Adv.*, 2015, **5**, 87416–87428.
34 A. P. Kulkarni, X. Kong and S. S. Jenekhe, *Adv. Funct. Mater.*, 2006, **16**, 1057–1066.
35 L. Yao, S. Sun, S. Xue, S. Zhang, X. Wu, H. Zhang, Y. Pan, C. Gu, F. Li and Y. Ma, *J. Phys. Chem. C*, 2013, **117**, 14189–14196.
36 Y. Li, X. L. Li, X. Cai, D. Chen, X. Liu, G. Xie, Z. Wang, Y. C. Wu, C. C. Lo, A. Lien, J. Peng, Y. Cao and S. J. Su, *J. Mater. Chem. C*, 2015, **3**, 6986–6996.
37 K. Shanmugasundaram, M. S. Subeesh, C. D. Sunesh, R. K. Chitumalla, J. Jang and Y. Choe, *J. Phys. Chem. C*, 2016, **120**, 20247–20253.
38 T. C. Chao, Y. T. Lin, C. Y. Yang, T. S. Hung, H. C. Chou, C. C. Wu and K. T. Wong, *Adv. Mater.*, 2005, **17**, 992–996.
39 A. D. Becke, *J. Chem. Phys.*, 1993, **98**, 5648–5652.
40 A. D. Becke, *J. Chem. Phys.*, 1996, **104**, 1040–1046.
41 C. Lee, W. Yang and R. G. Parr, *Phys. Rev. B: Condens. Matter Mater. Phys.*, 1988, **37**, 785–789.
42 Y. M. Wang, F. Teng, Y. B. Hou, Z. Xu, Y. S. Wang and W. F. Fu, *Appl. Phys. Lett.*, 2005, **87**, 233512.